Preparation of Porous Composite Bio-carriers from Lignin-Carbohydrate Complexes and Cellulose Nanocrystals, and their Application in the Culture of Human Hepatocytes

Hongfei Wu,[a] Yimin Xie,[a,b,*] Houkuan Zhao,[a] Xuekuan Chen,[a] Chen Jiang,[a] Shuying Bi,[a] and Yanchao Liu [a]

Lignin-carbohydrate complexes (LCC) were isolated from poplar wood after ball-milling for 48 h and 72 h. The water-insoluble LCC-48 and LCC-72 were fractionated. Porous spherical composite bio-carriers were prepared by liquid-nitrogen freezing using the water-insoluble LCCs and cellulose nanocrystals (CNC). Fourier transform infrared spectroscopy (FT-IR) showed that the bio-carriers were composed of lignin moieties and polysaccharide units. Scanning electron microscopy (SEM) revealed that the outer surface and cut surface of the spherical carrier had many pores. The specific surface areas of the LCC-72/CNC and the LCC-48/CNC composite carriers were 24.2 m^2/g and 28.9 m^2/g, respectively, while their pore sizes were 28.6 nm and 33.6 nm, respectively. Both carrier samples had good stability at pH 4.6 to 9.5 for about 50 days. Human hepatocytes were cultured *in vitro* with the bio-carriers and the cells grew well. A large number of cells adhered to the porous bio-carriers, and the cells of the experimental group to which the carriers were added exhibited higher metabolic activities. The CNC improved the biocompatibility for human hepatocytes. In summary, spherical bio-carriers prepared from LCC/CNC composite displayed high biocompatibility and have potential applications in liver tissue engineering.

Keywords: Lignin-carbohydrate complexes; Cellulose nanocrystals; Spherical carrier; Human hepatocytes; Biocompatibility

*Contact information: a: Research Institute of Pulp & Paper Engineering, Hubei University of Technology, 430068, Wuhan, China; b: Hubei Provincial Key Laboratory of Green Materials for Light Industry, Hubei University of Technology, 430068, Wuhan, China; *Corresponding author: ppymxie@163.com*

INTRODUCTION

The liver performs various essential functions for our survival, such as the control of plasma glucose levels, the synthesis of various proteins, including albumin and coagulation proteins, the synthesis of bile for the absorption of fat in the digestion process, detoxification by transaminase reactions, and the storage of several vitamins (Lee *et al.* 2016). However, liver disease afflicts over 10% of the world's human population. This includes chronic hepatitis, alcoholic steatosis, fibrosis, cirrhosis, and hepatocellular carcinoma (HCC). Although there are treatment options for most liver diseases, such as chemotherapy, injection of blood drugs, or surgery in some cases, many types are still incurable (Zhang *et al.* 2013). At present, the most effective medical treatment for liver diseases, such as liver cancer and acute liver failure, is liver

transplantation. The emergence of liver tissue engineering may offer a new therapy to solve the problem of insufficient liver donors. The purpose of liver tissue engineering is to construct a three-dimensional complex of hepatocytes and tissue materials to replace the diseased liver. Three important determinants to be considered in tissue engineering are the scaffold materials, seed cells, and growth regulators (Kulig and Vacanti 2004). Finding suitable scaffold materials has been one of the most important research areas of liver tissue engineering because of the basic performance of the artificial liver that mainly depends on the choice of scaffold material (Ghim *et al*. 2015). The available materials can be divided into two categories, namely natural scaffold materials and degradable polymer scaffold materials (Chung *et al*. 2002). A desirable scaffold material for liver tissue engineering must suit the following requirements: (1) have good biocompatibility and be non-toxic, bioactive, and degradable; (2) have good surface properties for cell adhesion growth; and (3) have a three-dimensional porous structure with a porosity of over 90% and retain appropriate mechanical strength (Chung and King 2011; Li *et al*. 2013).

Lignin-carbohydrate complexes (LCC) are a combination of hydrophobic lignin chemically bound to hydrophilic polysaccharides. Research on the connection of lignin and carbohydrates is still continuing. Within plant materials, the lignin and carbohydrates are combined by covalent bonds in LCC, and there are phenyl glycosidic bonds, ether bonds, and ester bonds between the lignin and the carbohydrates (Xie *et al*. 2000; Yuan *et al*. 2011; Nishimura *et al.* 2018). The polysaccharide fragment in the LCC is composed of various types of sugar units, such as glucose, arabinose, mannose, galactose, and a small amount of uronic acid (Jeffries 1990; Sakagami *et al*. 2005; Singh *et al*. 2005). Cell-wall polysaccharides containing 2% to 5% galactose moieties have the ability to recognize hepatocytes due to the presence of asialoglycoprotein receptors (ASGPR) on the hepatocytes, which binds to galactose (Cho *et al*. 2006; You *et al*. 2015; Roopan 2017). Uraki *et al*. (2004) prepared a temperature-sensitive gel by adding lignin and LCC. They found that the drug release temperature of the gel could be lowered because of the hydrophobic residual lignin structure. Zhao *et al.* (2017a) prepared a porous gel from LCC cross-linked with polyethylene glycol diglycidyl ether and successfully applied it for the culture of human hepatocytes; however, the polyethylene glycol diglycidyl ether was non-degradable.

Cellulose is the most abundant natural polymer available on the earth, and it is an important structural component of the cell wall of various plants. Apart from plants, cellulose is also present in a wide variety of living species, such as algae, fungi, bacteria, and even in some sea animals such as tunicates (Johnsy and Sabapathi 2015). When the width of a structure composed of parallel cellulose chains is below 100 nm, it could be called nanocellulose (Dufresne 2013). The nanocellulose has a large surface area and high strength. One important class of nanocellulose is obtained from renewable polymers by acid hydrolysis and has rod-like shape and revealed tunable surface chemistry (Liu *et al*. 2011). This kind of nanocellulose, called cellulose nanocrystals (CNC), has a large specific surface area, negative charge, and free hydroxyl groups. Therefore, as a tissue engineering material, CNC has the advantages of large specific surface area, good flexibility, and good biocompatibility (Jackson *et al*. 2011). In the preparation of tissue engineering scaffold materials, the addition of an appropriate amount of CNC could improve biocompatibility and mechanical strength.

In the present study, LCC/CNC porous spherical bio-carriers were prepared by mixing LCC and CNC, and freezing by liquid nitrogen, followed by freeze-drying

(Fig. 1). The structure of the composite was analyzed by Fourier transform infrared (FT-IR) spectra, and the carrier morphology was observed by scanning electron microscopy (SEM). Human liver cells L-02 were cultured with the LCC/CNC porous carriers. The biocompatibility of the porous carriers was analyzed by observation of the cell-growth status and detection of metabolic activities.

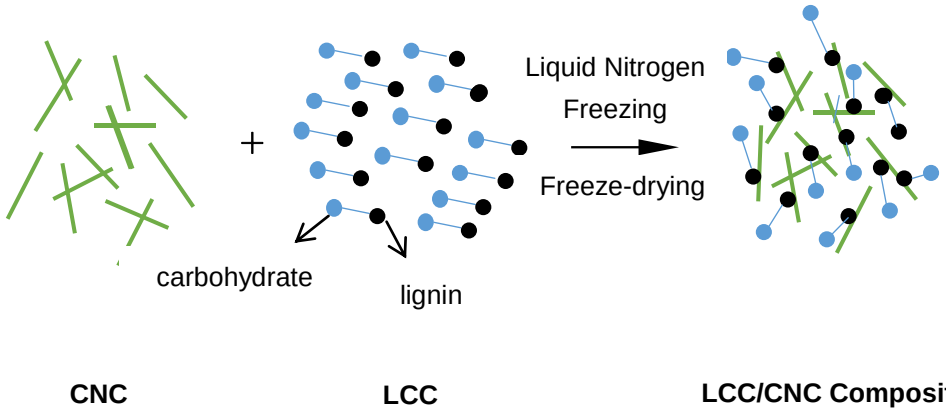

Fig. 1. Mechanism of the formation of LCC/CNC composite bio-carriers

EXPERIMENTAL

Materials

Poplar (*Populus euramericana*) wood was obtained from the Wuhan botanical garden (Wuhan, China). Human hepatocytes were provided by the Pricells Co. (Wuhan, China). The CNC suspension prepared from acid hydrolysis from cotton was purchased from Yuhan Technology Co. Ltd. (Hangzhou, China). Bovine insulin was purchased from Aladdin (Shanghai, China). Fetal bovine serum was purchased from Shanghai Yuanmu Biotechnology Co., Ltd. (Shanghai, China). A glucose kit was purchased from Nanjing Jiancheng Bioengineering Institute (Nanjing, China). Phosphate buffer saline was purchased from Shanghai Macklin Biochemical Technology Co., Ltd (Shanghai, China).

Methods

Preparation of poplar LCC

Poplar wood chips were ground with a Wiley mill (FZ102, Tianjin Taishite, China) and then extracted with benzene-ethanol mixture (2/1, V/V). The powder was completely dried *in vacuo* for about one week. The dry wood powder was then ground for 48 h and 72 h, respectively, using a water-cooled vibratory ball-mill (MB-0, Chuo-koki.Co. Ltd, Japan). The milled sample was extracted three times using dioxane-water solution (96/4, V/V). An insoluble material was obtained after centrifugation, which was then extracted with a mixture of acetic acid and water (1/1, V/V). The material obtained after removing the solvents was then purified using the Björkman method to obtain LCC sample (Björkman 1957).

Separation of water-insoluble LCC

About 0.5 g of poplar LCC and 50 mL of distilled water were put into a 100-mL

Erlenmeyer flask, heated to 50 °C, and stirred for 8 h. The precipitate obtained was collected by centrifugation and then freeze-dried (-85 °C, 0.006 Torr) to obtain the water-insoluble poplar LCC.

Preparation of LCC/CNC composite spherical bio-carriers

The water-insoluble LCCs (LCC-48 and LCC-72) were dissolved in 85% acetic acid solution, and the solution was poured into a 30-mL Erlenmeyer flask containing CNC suspension with stirring at room temperature. The mass fraction of LCCs and CNC used for various samples were 0%/100%, 10%/90%, 20%/80%, 30%/70%, 50%/50%, 60%/40%, 70%/30%, and 100%/0%, respectively. The mixture of LCC/CNC was then slowly added dropwise to liquid nitrogen using a sterile syringe. The spherical bio-carriers were prepared by freeze-drying (-85 °C, 0.006 Torr) the mixture of LCC/CNC.

FT-IR spectroscopy

The LCC/CNC bio-carrier sample (about 1.0 mg) was mixed with 300 mg KBr *via* grinding. The ground powder was then pressed into a pellet. The KBr-pellet sample was analyzed using an FT-IR spectrometer (Thermofisher 6700, USA).

Observation of the surface morphology of spherical bio-carriers by SEM

The LCC/CNC composite spherical bio-carriers were put on a silicon wafer and treated by sputter coating *in vacuo*. The surface and cut surface morphology of the composite carriers was observed by SEM (JSM-6390LV, Tokyo, Japan).

Determination of specific surface area and pore size of the bio-carriers

The specific surface area and pore size of the spherical bio-carrier samples were determined using a BELSORP-mini II type (Ankersmid, Netherlands) high-precision surface area and pore size analyzer.

Determination of stability of the spherical carriers

The LCC/CNC composite carrier samples were allowed to soak in various buffer solutions in a 50-mL Erlenmeyer flask, *i.e.*, acetic acid buffer (pH 4.6), phosphate buffer (pH 7.0), and $NaHCO_3$ buffer (pH 9.5) for 50 days at room temperature. After removing the buffer, the morphology of the bio-carrier samples was observed with an optical microscope (Olympus SZX16, Japan).

Culture of human hepatocytes

Human hepatocytes (L-02) obtained from Pricells Co. (Wuhan, China) were rinsed with phosphate buffer. The hepatocytes were then inoculated into 12-well culture plates at a density of 3×10^5 cells/mL. The bio-carriers were sterilized in dry state at 120 °C for 4 h. These were then added to the wells at a concentration of 2.5 mg/mL. The hepatocytes, together with the bio-carriers, were incubated at 37 °C, 5% CO_2, and 100% relative humidity. The culture medium (RPMI-1640) was supplemented with 20% FBS (fetal bovine serum), 1% penicillin, and streptomycin solution. The adhesion of human hepatocytes to the spherical bio-carriers was observed daily using a Leica DM-6000 CS microscope (Leica Instruments Inc., Wetzlar, Germany). Cell-free supernatant was collected by centrifugation daily to detect the metabolic activity of the cells.

Calculating the cell number

For one week of the culture of human hepatocytes (L-02), the liquid media were collected every day in a clean bench, and the cells were washed twice with phosphate buffer followed by 0.25% trypsin digestion for 1 min to 2 min.

After the digestive medium was removed, new medium was added to terminate the digestion. The cells were dissociated into a single cell suspension. Cell suspensions (200 μL) were stained with 0.4% trypan blue solution and placed on a hemacytometer for counting on a Leica DM-6000 CS microscope (Leica Instruments Inc., Wetzlar, Germany).

SEM observation of the spherical bio-carriers

The porous carriers were taken out on the fifth day of the human liver cell culture. The cells on the porous carriers were fixed with 200 μL glutaraldehyde solution (2.5%, w/w) and then fixed with 200 μL osmic acid (10 g/L) for 5 h. After washing three times with 3 mL phosphate buffer solution (pH 7.4), the obtained cells were dehydrated with different concentrations of ethanol for 15 min.

The bio-carriers were then dried *in vacuo*. The dried porous bio-carriers were treated by sputter coating *in vacuo*. Then the cell-attached carriers were observed by SEM and photographed.

Detection of metabolic activity of the cultured human hepatocytes

Cell-free supernatant (10 μL), standard albumin (10 μL), and distilled water (10 μL) were added to a centrifuge tube. After the addition of 2.5 mL bromocresol green buffer, the samples were shaken to complete the reaction. The absorption values were monitored at 628 nm using a UV spectrophotometer (UV-2550, SHIMADZU, Japan) (Zhao *et al*. 2017b). The following equation (Eq. 1) was used for calculating the albumin content,

$$ALB\ (g/L) = \frac{A_1 - A_0}{A_2 - A_0} \times C_0 \quad (1)$$

where *ALB* is the content (g/L) of albumin; A_1 denotes the absorbance of the sample solution; A_2 is the absorbance of the standard solution; C_0 represents the concentration (g/L) of the standard albumin solution; and A_0 is the absorbance of distilled water.

Cell-free supernatant (10 μL), 10 mmol/L blood urea nitrogen standard solution (10 μL), and distilled water (10 μL) were added to a centrifuge tube. After 15 μL oxime solution (1 g/L) and 15 μL sulfuric acid solution (0.2 g/L) were added to the centrifuge tube, the mixture was mixed, placed in boiling water for 15 min, and then cooled with cold water. The absorption values were monitored at 628 nm. Equation 2 was used for calculating the blood urea nitrogen content,

$$BUN\ (mmol/L) = \frac{A_1 - A_0}{A_2 - A_0} \times C_0 \quad (2)$$

where *BUN* is the content (mmol/L) of blood urea nitrogen; A_1 is the absorbance of the sample solution; A_2 is the absorbance of the standard solution; C_0 is the concentration (g/L) of the standard blood urea nitrogen solution; and A_0 is the absorbance of distilled water.

About 10 μL of distilled water, 10 μL standard glucose, and 10 μL cell-free supernatant were taken in a test tube. Then, 15 μL peroxidase buffer solution (1 U/mL),

glucose oxidase solution (10 U/mL), and a mixture of 1,5 dimethyl-2-phenyl-4-amino-3-pyrazolone (70 mmol), and phenol (10.6 mmol/L) were added. The mixture was mixed and allowed to react completely. The absorption values were monitored at 505 nm, and the following Eq. 3 was used for calculating the glucose content,

$$C\ （mmol/L）= \frac{A_1}{A_2} \times C_0 \quad (3)$$

where C is the content (mmol/L) of glucose; A_1 is the absorbance of the sample solution; A_2 is the absorbance of the standard solution; and C_0 is the concentration (g/L) of the glucose standard solution.

RESULTS AND DISCUSSION

FT-IR Analysis and Composition Elucidation

The FT-IR spectra of the LCC/CNC spherical carriers prepared from 48 h and 72 h ball-milling times (LCC/CNC with an LCC mass fraction of 60% is used as an example) are shown in Fig. 2.

The tentative peak assignment is shown in Table 1. From the spectra, the characteristic peaks of the LCC/CNC bio-carriers prepared by different ball-milling times were similar and displayed typical chemical structures of lignin and carbohydrates, including cellulose. From the absorption peak at 1738.1 cm^{-1} to 1732.2 cm^{-1}, it can be concluded that there was a non-conjugated C=O group in the LCC. The strong absorption peak at 1045.3 to 1045.7 cm^{-1} in the spectra of the LCC/CNC composite is due to the C-O stretching of the polysaccharides, including cellulose of CNC and hemicellulose in LCC (Fan *et al*. 2006). These results indicated that the LCC/CNC bio-carriers consisted of lignin moieties and sugar units from the polysaccharide.

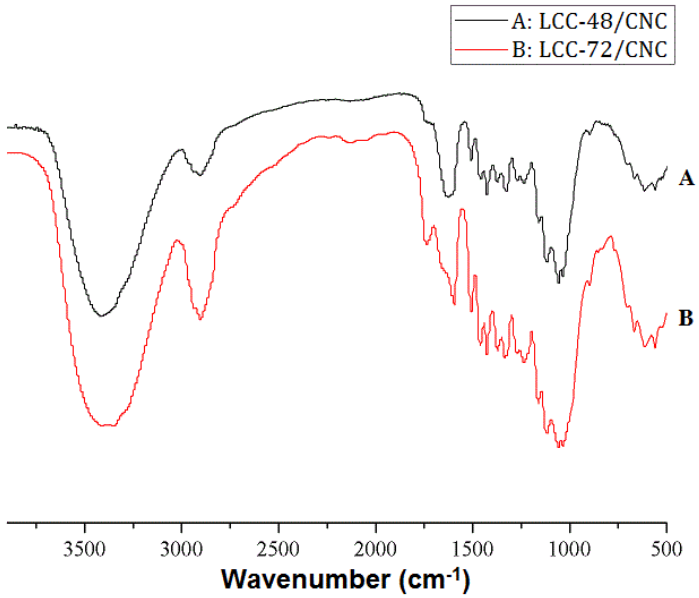

Fig. 2. FT-IR spectroscopy of LCC/CNC composite spherical bio-carriers. A: LCC-48/CNC; B: LCC-72/CNC

Table 1. Tentative Analysis of the Main Absorption Peaks of Composite Bio-carriers

Wave number (cm^{-1})		Functional Group Attribution	Reference
LCC-48/CNC	LCC-72/CNC		
3419.8	3414.6	O-H stretching vibration	Tang *et al*. 2014
2920.6	2918.7	Stretching vibrations of C-H in $-CH_3$, $-CH_2$, and –CH groups	Zhang *et al*. 2017 Zaman *et al*. 2012
1732.7	1723.9	-C=O unconjugated	You *et al*. 2015
1610.9 1511.5	1601.6 1512.3	Aromatic ring in lignin Aromatic ring in lignin	Naumann *et al*. 2005 Durmaz *et al.* 2016
1456.6	1455.4	C-H stretching vibration in $-CH_3$	Hon *et al*. 2000
1422.0	1416.7	Vibration of aromatic ring	You *et al*. 2015
1367.9	1373.4	Aromatic –O-H vibration	Hon *et al.* 2000
1271.3	1270.9	Aromatic methoxy -C-O vibration	Hon *et al*. 2000
1142.2	1133.6	Aromatic -C-H vibration (G- or S-type lignin monomer)	Zaman *et al*. 2012
1040.03	1037.96	C-O stretching vibrations in cellulose and hemicellulose	Durmaz *et al*. 2016 Fan *et al*. 2006
875.12	874.93	C-H in glycosidic linkages	Zaman *et al*. 2012

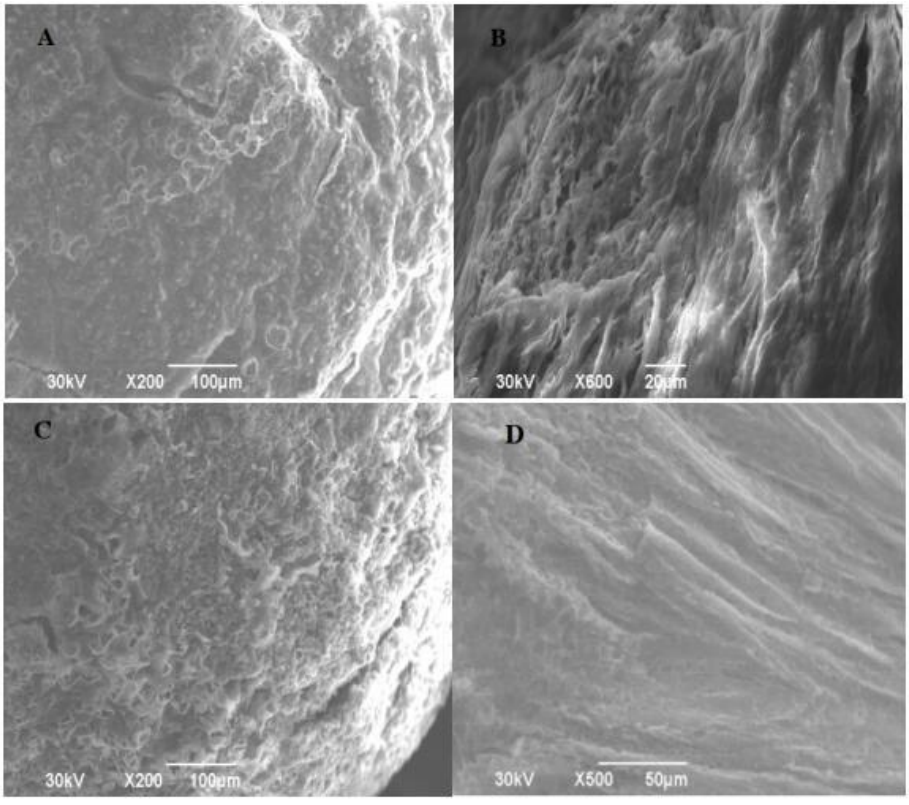

Fig. 3. SEM images of spherical bio-carriers: A: Surface of LCC-48/CNC; B: Cut surface of LCC-48/CNC; C: Surface of LCC-72/CNC; and D: Cut surface of LCC-72/CNC

SEM Images of Spherical Bio-carriers

Figure 3 shows the surface and cut surface of the LCC/CNC bio-carriers with different ball-milling times as observed by SEM (LCC/CNC with an LCC mass fraction

of 60% was used as an example). There were many holes and cracks on the surface of the LCC/CNC bio-carriers. After the carriers were cut radially, there were many holes and gullies within the carriers, which provided suitable space for cell growth.

Analysis of Specific Surface Area and Pore Diameter

The specific surface area and pore size of the composite bio-carriers were determined by BET analysis with liquid nitrogen at -196 °C followed by degassing at 130 °C (Wellner *et al*. 1998; Chirkova *et al*. 2011). The specific surface area of the bio-carriers was calculated using Eq. 4,

$$S_g = 4.36 \times V_m/W \quad (4)$$

where S_g is the specific surface area (m^2/g) of the sample powder; V_m is the nitrogen monolayer adsorption saturation (mL); W is the sample weight (g). The average pore size of the bio-carriers was calculated by Eq. 5,

$$R_k = -0.414/\log (P/P_0) \quad (5)$$

where R_k is the Kelvin radius (μm); P is liquid nitrogen's partial pressure (Pa); and P_0 is the saturated vapor pressure (Pa) of nitrogen at liquid nitrogen temperature.

The results for the average pore diameter and specific surface area are shown in Figs. 4 and 5, respectively. The specific surface areas of the LCC-72/CNC and the LCC-48/CNC bio-carriers were determined to be 24.2 m^2/g and 28.9 m^2/g, respectively. The average pore diameters measured were 28.6 nm and 33.6 nm, respectively. These results showed that the LCC/CNC composite bio-carriers had an appropriate pore size and enough specific surface area suitable for use in the culture of hepatocytes.

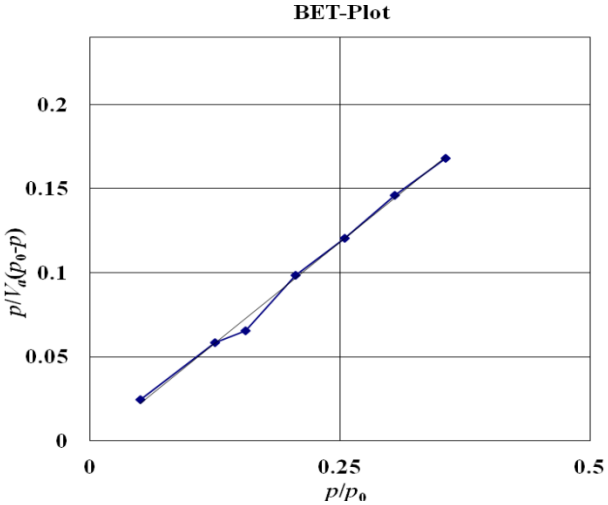

Fig. 4. BET adsorption isotherm of LCC-48/CNC bio-carriers

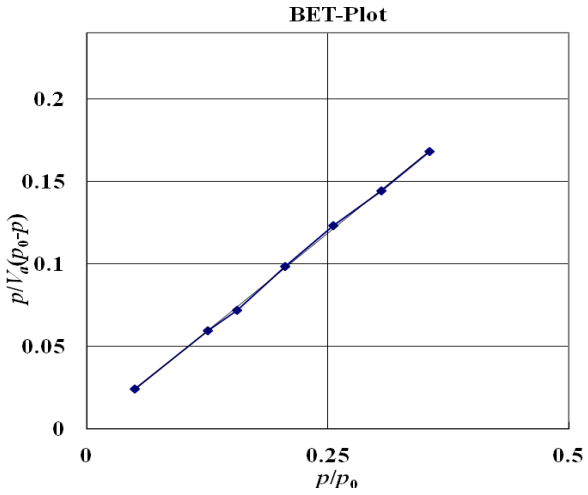

Fig. 5. BET adsorption isotherm of LCC-72/CNC bio-carriers

Stability Analysis of Spherical Bio-carriers

The stability analysis was conducted by immersing the bio-carriers in solutions of various pH values followed by measuring the change in size. The temperature of the solution was always maintained at 37 °C. As shown in Table 2, the there was no alteration in the size of the LCC/CNC bio-carriers in a wide range of pH values for 50 days in weak acid, weak alkali, and neutral medium.

Therefore, it could be concluded that the spherical carriers had excellent stability. In addition, the experiment also revealed that although CNC crystal had a certain hydrophilicity, once it became a xerogel together with water-insoluble LCC, it posed some resistance to water and maintained its original size. This may also be related to the poor water accessibility of the cellulose crystal in the CNC.

Table 2. Size Change of Spherical Bio-carriers in Various pH Conditions for 50 Days

Carrier sample	Diameter (cm)			
	Dry State	pH 4.6	pH 7.4	pH 9.5
LCC-48/CNC	1.8–2.0	1.9–2.1	1.9–2.1	1.9–2.1
LCC-72/CNC	1.8–2.0	1.9–2.1	1.9–2.1	1.9–2.1

The Growth of the Human Hepatocytes

The results of cell counting on days one to seven are shown in Figs. 6 and 7. Upon comparison with the cells cultured using the LCC/CNC spherical carriers and the cells cultured in the control solution showed an increased growth for the first 5 days, although the growth rate of the cells for the first 4 days was relatively slow. The number of hepatocytes formed was the highest on the 5th day, after which the number of cells began to decrease gradually. The cell-growth trend was as follows: LCC-72/CNC (50% LCC) > LCC-48/CNC (50% LCC)> CNC > control group. It was clear that the addition of CNC indicated some compatibility with human hepatocytes although the effect was weaker than that of LCC.

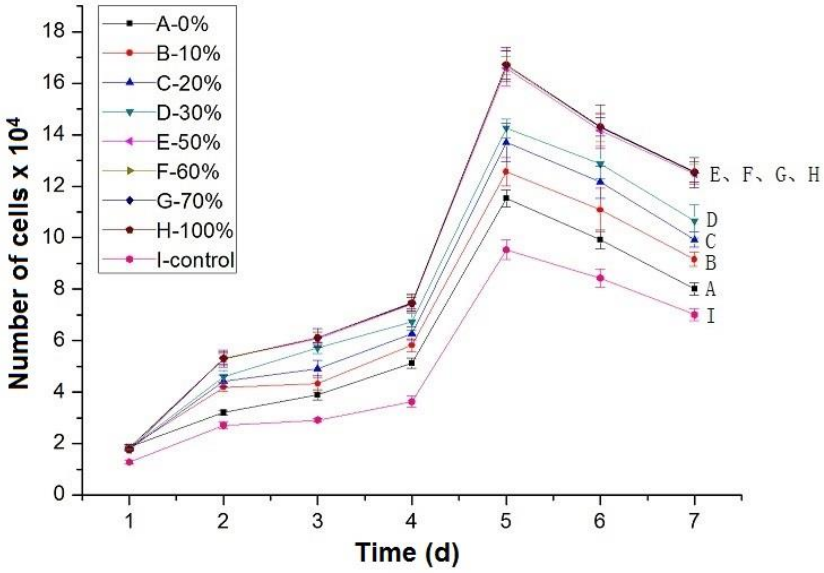

Fig. 6. Hepatocyte counting curves for cells cultured *in vitro* on LCC-48/CNC composite-based bio-carriers with various contents of LCC – 0% to 100%: LCC content in bio-carriers prepared from LCC/CNC mixture; and I: control experiment without bio-carriers

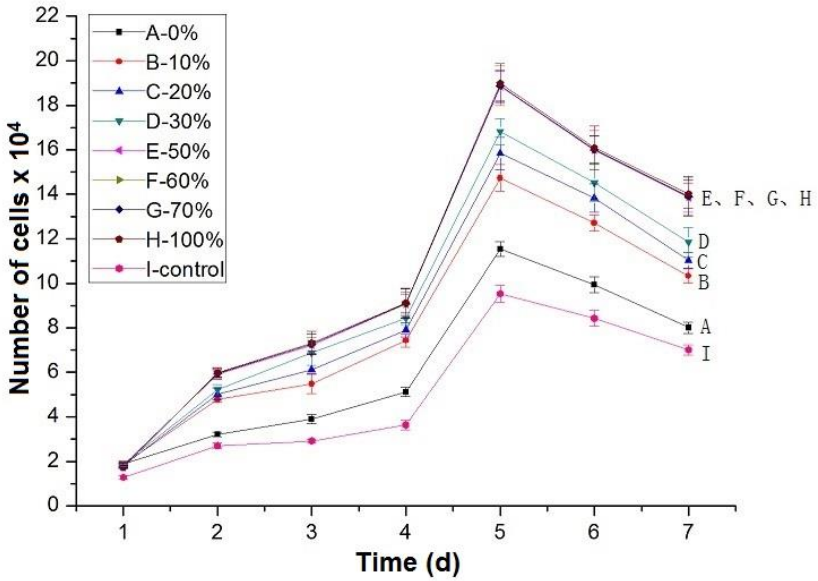

Fig. 7. Hepatocyte counting curves for cells cultured *in vitro* on LCC-72/CNC composite-based bio-carriers with various contents of LCC – 0% to 100%: LCC content in bio-carriers prepared from LCC/CNC mixture; and I: control experiment without bio-carriers

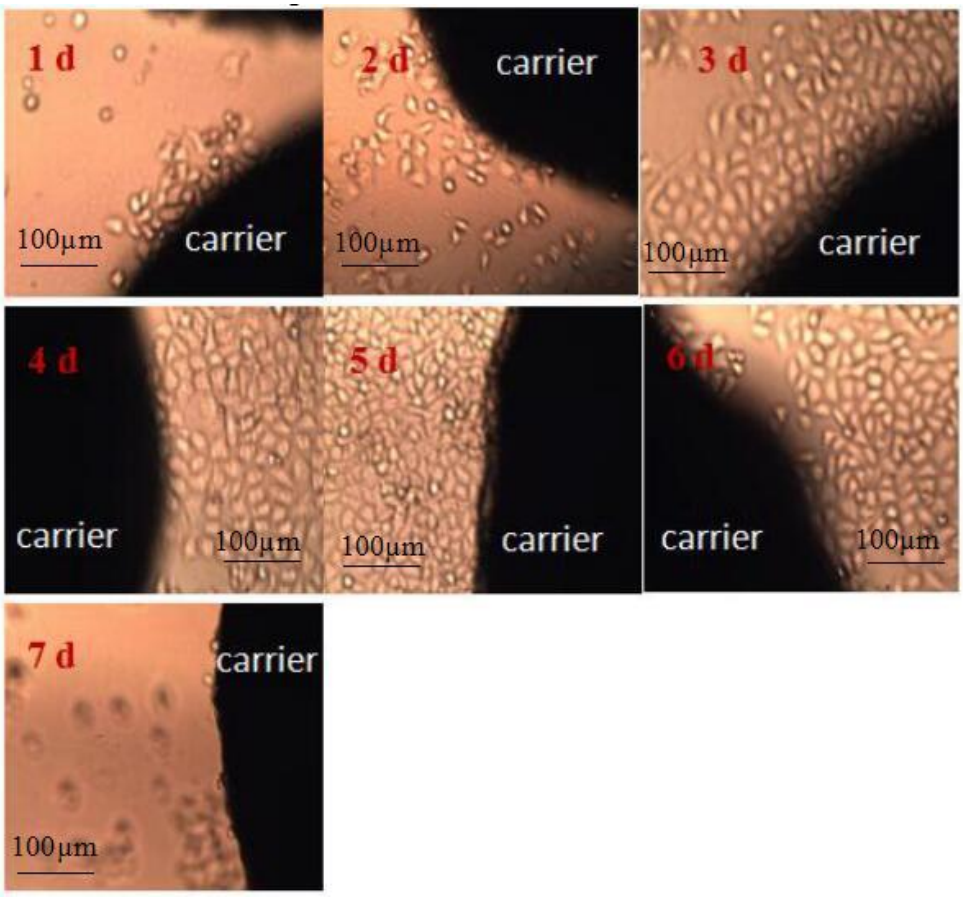

Fig. 8. Hepatocyte adhesive growth on LCC-48/CNC spherical carriers (First to seventh day)

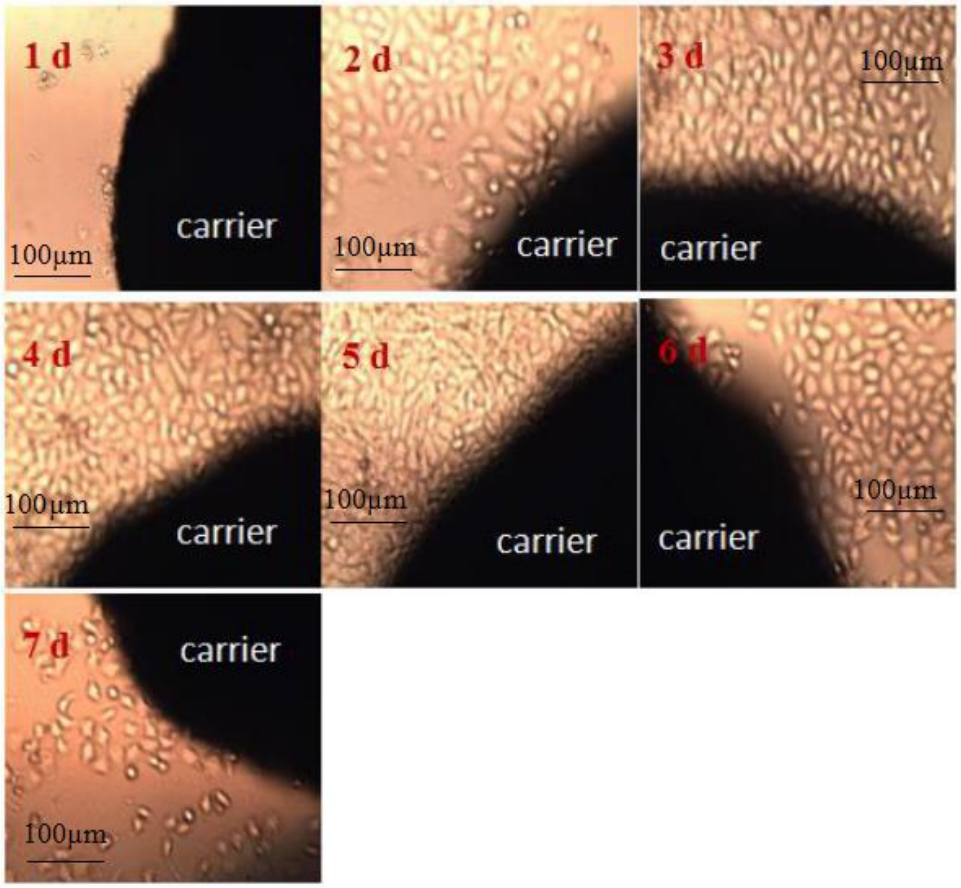

Fig. 9. Hepatocyte adhesive growth on LCC-72/CNC spherical carriers (First to seventh day)

Wang *et al*. (2015) found that the doping of biocompatible nanomaterials into ultrahigh molecular weight polyethylene (UHMWPE) to improve the biocompatibility and to reduce the wear-debris is of great significance to prolonging implantation time of UHMWPE as the bearing material for artificial joints. Wang *et al.* (2009) also found that the nano-bacterial cellulose co-culture composition was well integrated into the skin of nude mice. Thus, it is natural to conclude that nano-bacterial cellulose was beneficial to cell attachment and proliferation under these conditions.

When the content of LCC in the bio-carriers was less than 50%, the number of cells increased with enhancement of the content of LCC. When the content of LCC in LCC/CNC exceeded 50%, the number of cells no longer increased as the content of LCC was increased.

Figures 8 and 9 show the growth of cells on the LCC-48/CNC and LCC-72/CNC spherical carriers with an LCC mass fraction of 60%. Among them, the rate of growth was the fastest on the 5th day, and the cells began apoptosis from the 6th day. The cells grew around the carriers adhesively, which indicated that the cells could recognize and bind to the carriers that had good biocompatibility. These results were in agreement with that of Zhao *et al.* (2017a). Nwe *et al*. (2010) used a confocal laser microscope to observe 6th-day-old NIH/3T3 fibroblasts grown on a nano-bacterial cellulose membrane and found that the cell could grow well on the membrane.

Scanning Electron Microscopy

The SEM images on day 5 of the liver cell culture on LCC/CNC bio-carriers are shown in Fig. 10. The Figs. 10-A and 10-B showed the adhesion of liver cells on the LCC-48/CNC and LCC-72/CNC porous carriers, respectively. The liver cells could attach to the LCC/CNC porous carriers and the number of cells growing on the LCC-72/CNC composite carriers was considerably larger than that of cells on the LCC-48/CNC composite carriers. These data indicated that the LCC-72/CNC bio-carriers were more favorable for the growth of liver cells. This result was in good agreement with the observation of human hepatocytes cultured on spherical bio-carriers prepared with LCC isolated from ginkgo (*Ginkgo biloba* L.) xylem (Zhao *et al*. 2017b).

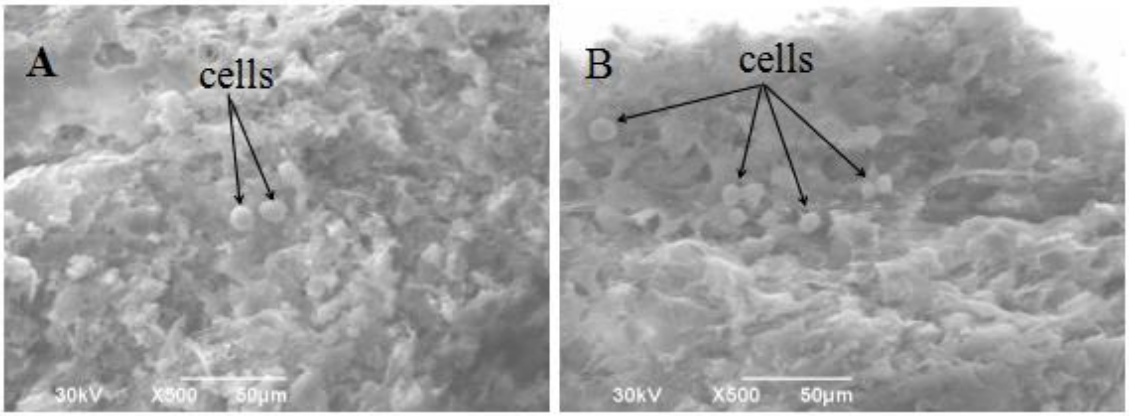

Fig. 10. SEM images of human hepatocytes adhering to LCC/CNC spherical bio-carriers. A: LCC-48/CNC; and B: LCC-72/CNC

Detection of Metabolic Activity of Human L-02 Hepatocytes

Determination of ALB content

In Figs. 11 and 12, the content of albumin (ALB) secreted by the hepatocytes cultured on the experimental and the control groups increased during the first 5 days. On the 5th day, the content of ALB reached a peak value and then it gradually decreased from the 6th day.

In the experimental group using LCC/CNC porous bio-carriers, the ALB contents were substantially higher than those in the control group. As the content of LCC increased, the value of ALB content initially increased and then remained unchanged. The ALB content remained unchanged when the content of LCC was more than 50%. The hepatocytes cultured on the LCC-72/CNC porous carriers had higher ALB contents than that of the LCC-48/CNC porous carriers. The contents of ALB secreted by the hepatocytes cultured on the LCC-72/CNC, LCC-48/CNC, CNC, and control groups on the 5th day were 16.13 g/L, 15.82 g/L, 9.17 g/L, and 7.17 g/L, respectively. These results showed that cells cultured with the LCC bio-carrier samples had a higher metabolic activity than that cultured with CNC alone. Zhao *et al.* (2017a) also found LCC-72 from poplar wood led to a higher ALB value than that of LCC-48 sample. From the results of the present experiment, the ALB values of LCC-72/CNC and LCC-48/CNC were higher than the corresponding LCC. These results indicated that the CNC could improve the biocompatibility of the spherical bio-carriers.

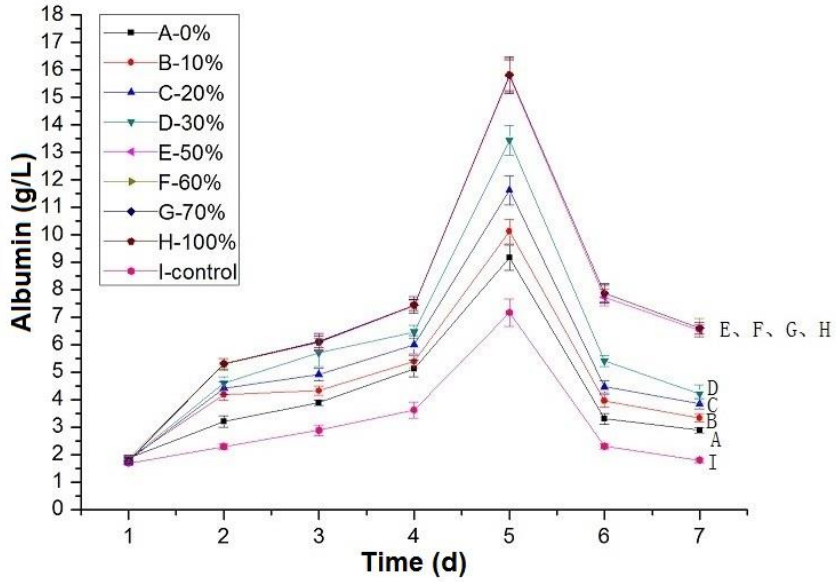

Fig. 11. Content of ALB from hepatocytes cultured on LCC-48/CNC composite-based bio-carriers with various contents of LCC – 0% to 100%: LCC content in bio-carriers prepared from LCC/CNC mixture; and I: control experiment without bio-carrier

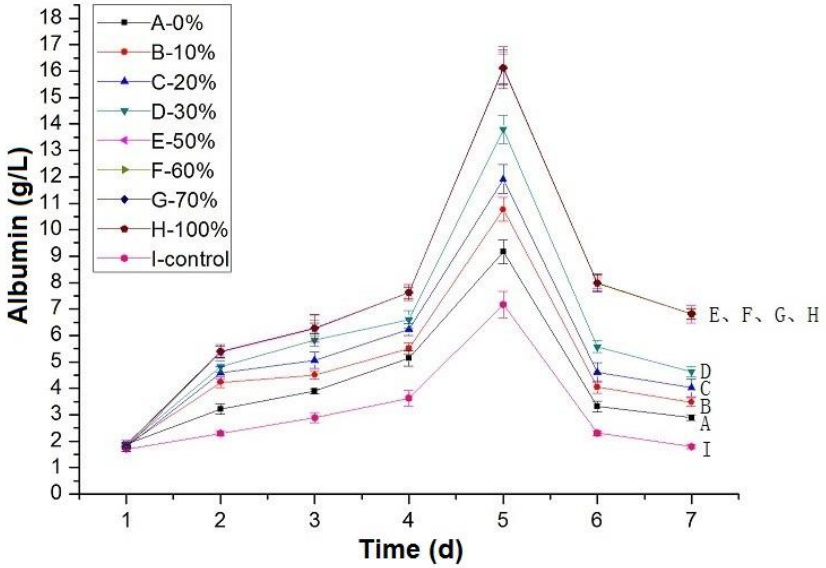

Fig. 12. Content of ALB from hepatocytes cultured on LCC-72/CNC composite-based bio-carriers with various contents of LCC – 0% to 100%: LCC content in bio-carriers prepared from LCC/CNC mixture; and I: control experiment without bio-carriers

Determination of BUN content

As shown in Figs. 13 and 14, the contents of blood urea nitrogen (BUN) measured in the experimental and control groups increased during the first 5 days. On the 5th day,

the content of BUN reached its maximum value and then it gradually decreased from the 6th day. The BUN levels in the experimental groups with the LCC/CNC bio-carriers were considerably higher than those of the control group.

As the content of LCC increased, the value of BUN initially increased and then remained unchanged. After the content of LCC reached 50%, the BUN value remained unchanged. The value of BUN secreted by cells cultured in the LCC-72/CNC porous carriers was higher than that of the LCC-48/CNC porous carrier culture. The value of BUN for LCC-72/CNC, LCC-48/CNC, CNC, and control group peaked on the 5th day, with the highest values being 2.98 mmol/L, 2.83 mmol/L, 1.17 mmol/L, and 0.97 mmol/L, respectively.

These results showed that cells cultured with LCC/CNC bio-carriers had high metabolic activity. Galactosylated substrates as LCC are suitable biomaterials in the preparation of scaffolds for hepatocytes cultivation because of their specific interaction of the galactose moiety with the asialoglycoprotein receptor (ASGPR) of the cell-surface (Geffen and Spiess 1993). Moreover, Chen *et al.* (2006) prepared samples of lignin/chitosan composite membranes for use as surgical sutures and showed that lignin had good biocompatibility. Because the porous spherical carrier prepared in this research work contains a large amount of lignin and polysaccharide components, it has high biocompatibility.

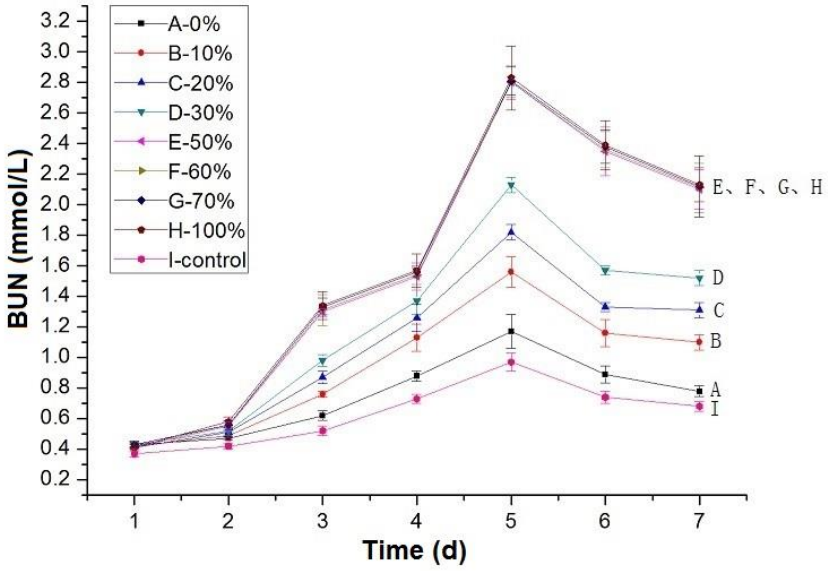

Fig. 13. The BUN levels from hepatocytes cultured on LCC-48/CNC composite-based bio-carriers with various contents of LCC – 0% to 100%: LCC content in bio-carriers prepared from LCC/CNC mixture; and I: control experiment without bio-carriers

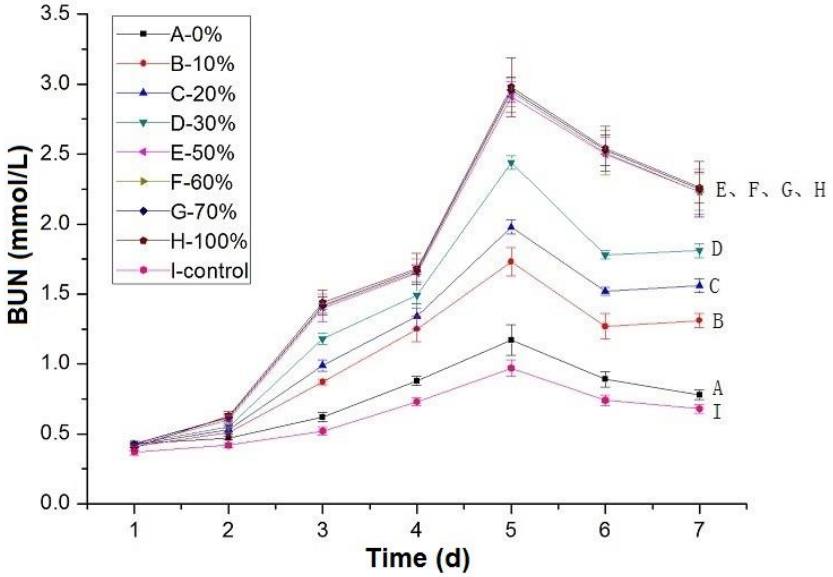

Fig. 14. The BUN levels from hepatocytes cultured on LCC-72/CNC composite-based bio-carriers with various contents of LCC – 0% to 100%: LCC content in bio-carriers prepared from LCC/CNC mixture; and I: control experiment without bio-carriers

Determination of glucose consumption

As shown in Figs. 15 and 16, the consumption of glucose in the experimental and the control groups increased during the first 5 days.

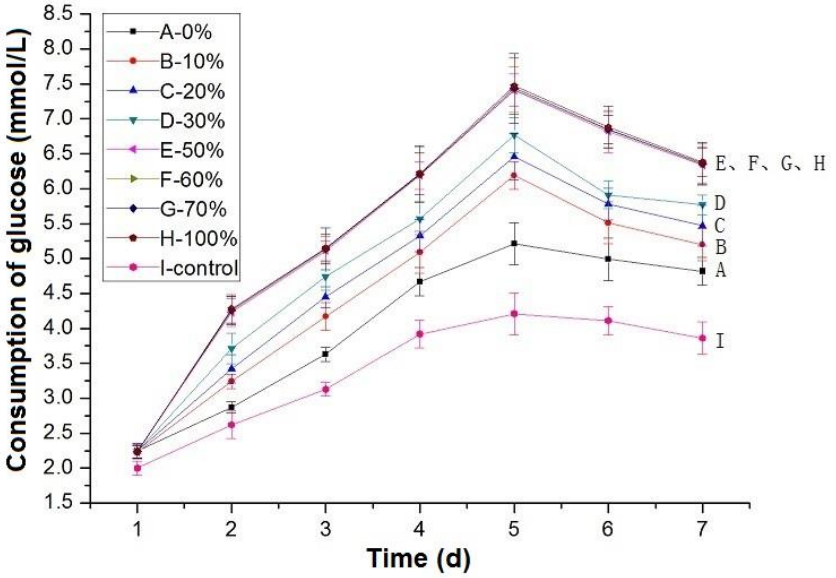

Fig. 15. Consumption of glucose by hepatocytes cultured on LCC-48/CNC composite-based bio-carriers with various contents of LCC – 0% to 100%: LCC content in bio-carriers prepared from LCC/CNC mixture; and I: control experiment without bio-carrier

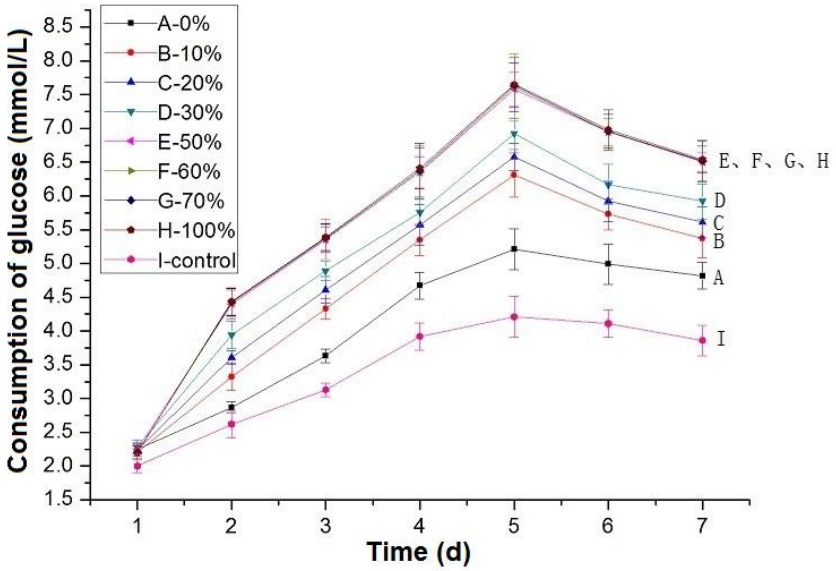

Fig. 16. Consumption of glucose by hepatocytes cultured on LCC-72/CNC composite-based bio-carriers with various contents of LCC – 0% to 100%: LCC content in bio-carriers prepared from LCC/CNC mixture; and I: control experiment without bio-carrier

On the 5th day, the consumption of glucose peaked, and then it gradually decreased from the 6th day. Moreover, the consumption of glucose in the experimental group with LCC/CNC bio-carriers was considerably higher than that of the control group. When the content of LCC in LCC/CNC was less than 50%, the consumption of glucose increased as the content of LCC increased. When the content of LCC in LCC/CNC was higher than 50%, the consumption of glucose no longer increased with the enhancement of LCC content. The consumption of glucose in the experiment with LCC-72/CNC, LCC-48/CNC, CNC, and control groups on the 5th day was 7.65 mmol/L, 7.47 mmol/L, 5.21 mmol/L, and 4.21 mmol/L, respectively. The consumption of glucose in the LCC-72/CNC porous carriers was higher than that in the LCC-48/CNC porous carriers. These results showed that cells cultured with the LCC/CNC bio-carriers had high metabolic activity.

CONCLUSIONS

1. The bio-carriers were analyzed by FT-IR spectrometry and found to contain lignin moieties and polysaccharide units. A large amount of lignin and polysaccharide structure provides excellent biocompatibility of LCC-48/CNC and LCC-72/CNC composite spherical carriers.
2. The LCC-48/CNC and LCC-72/CNC composite bio-carriers showed a large number of internal and external pores with many obvious gullies, which provided a good three-dimensional environment for the biological carriers. The LCC-48/CNC and LCC-72/CNC composite bio-carriers had different porosities and pore diameters. The porosity of LCC-72/CNC and LCC-48/CNC composite spherical carriers was

high. Both had good stability at pH 4.6 to 9.5 for 50 days.

3. Human hepatocytes were cultured *in vitro* using the LCC/CNC spherical bio-carriers. The analysis of cell morphology and the metabolic activities of the hepatocytes indicated that, the bio-carriers were biocompatible and could enhance the growth of hepatocytes adhered to the carriers. The compatibility sequence was as follows: LCC-72/CNC > LCC-48/CNC > CNC > control group. The biocompatibility of bio-carriers with human hepatocytes was enhanced by adding CNC.
4. The biocompatibility of the bio-carriers was enhanced with increasing the LCC content. Once the LCC content reached 50%, its biocompatibility remained unchanged. The results showed that the porous biomaterials prepared from water-insoluble poplar-LCC and CNC exhibited excellent biocompatibility and may have potential as a liver tissue engineering scaffold material.

ACKNOWLEDGMENTS

The authors are grateful for the financial support of the Nature Science Foundation of China (grant No.21878070) and the Hubei Provincial Key Laboratory of Green Materials for Light Industry (Q20131402).

REFERENCES CITED

Björkman, A. (1957). "Lignin and lignin-carbohydrate complexes," *Industrial and Engineering Chemistry* 49(9), 1395-1398. DOI: 10.1021/ie50573a040

Chen, X. G., Liu, C. S., Liu, C. G., Meng, X. H., Chong, M. L., and Park, H. J. (2006). "Preparation and biocompatibility of chitosan microcarriers as biomaterial," *Biochemical Engineering Journal* 27(3), 269-274. DOI: 10.1016/j.bej.2005.08.021

Chirkova, J., Andersone, I., Irbe, I., Spince, B., and Andersons, B. (2011). "Lignins as agents for bio-protection of wood," *Holzforschung* 65(4), 497-502.

Cho, C. S., Seo, S. J., Park, I. K., Kim, S. H., Kim, T. H., Hoshiba, T., Harada, I., and Akaie, T. (2006). "Galactose-carrying polymers as extracellular matrices for liver tissue engineering," *Biomaterials* 27(4), 576-585. DOI: 10.1016/j.biomaterials.2005.06.008

Chung, S., and King, M. W. (2011). "Design concepts and strategies for tissue engineering scaffolds," *Biotechnology and Applied Biochemistry* 58(6), 423-438. DOI: 10.1002/bab.60

Chung, T. W., Yang, J., Akaike, T., Cho, K. Y., Nah, J. W., Kim, S. I., Cho, C. S. (2002). "Preparation of alginate/galactosylated chitosan scaffold for hepatocyte attachment," *Biomaterials* 23(14), 2827-2834. DOI: 10.1016/S0142-9612(01)00399-4

Dufresne, A. (2013). "Nanocellulose: A new ageless bionanomaterial," *Materials Today* 16(6), 220-227. DOI: 10.1016/j.mattod.2013.06.004

Durmaz, S., Özlem, Ö., Boyaci, I. H., Yildiz, U. C., and Erisir, E. (2016). "Examination of the chemical changes in spruce wood degraded by brown-rot fungi using FT-IR and FT-Raman spectroscopy," *Vibrational Spectroscopy 85*, 202-207. DOI: 10.1016/j.vibspec.2016.04.020

Fan, Z., Chen, J., Wang, M., Cui, K., Zhou, H., and Kuang, Y. (2006). "Preparation and characterization of manganese oxide/CNT composites as supercapacitive materials," *Diamond and Related Materials* 15(9), 1478-1483. DOI: 10.1016/j.diamond.2005.11.009

Geffen, I., and Spiess, M. (1993). "Asialoglycoprotein receptor," *International Review of Cytology* 137(137B), 181-219. DOI: 10.1007/978-1-4612-0477-0_21

Ghim, J. H., Hussein, K. H., Park, K. M., and Woo, H. M. (2015). "Hepatic cell encapsulation using a decellularized liver scaffold," *Biomedical Engineering Letters* 5(1), 58-64. DOI: 10.1007/s13534-015-0176-0

Hon, D., and Shiraishi, N. (2000). *Wood and Cellulosic Chemistry*, Revised and Expanded, CRC Press, Florida, USA

Jackson, J. K., Letchford, K., Wasserman, B. Z., Ye, L., Hamad, W. Y., and Burt, H. M. (2011). "The use of nanocrystalline cellulose for the binding and controlled release of drugs," *International Journal of Nanomedicine* 6(6), 321-330.DOI: 10.2147/IJN.S16749

Jeffries, T. W. (1990). "Biodegradation of lignin-carbohydrate complexes," *Biodegradation* 1(2-3), 163-176. DOI: 10.1007/BF00058834

Johnsy, G., and Sabapathi, S. N. (2015). "Cellulose nanocrystals: Synthesis, functional properties, and applications," *Nanotechnology, Science and Applications*8, 45–54. DOI: 10.2147/NSA.S64386

Kulig, K. M., and Vacanti, J. P. (2004). "Hepatic tissue engineering," *Transplant Immunology* 12(3), 303-310. DOI:10.1016/j.trim.2003.12.005

Lee, J. W., Choi, Y. J., Yong, W. J., Pati, F., Shim, J. H., Kang, K. S., Kang, I. H., Park, J., and Cho, D. W. (2016). "Development of a 3D cell printed construct considering angiogenesis for liver tissue engineering,"*Biofabrication* 8(1), 015007. DOI: 10.1088/1758-5090/8/1/015007

Li, Y. S., Harn, H. J., Hsieh, D. K., Wen, T. C., Subeq, Y. M., Sun, L. Y., Lin, S. Z., Chiou, T. W. (2013). "Cells and materials for liver tissue engineering," *Cell Transplantation* 22(4), 685-700. DOI: 10.3727/096368912X655163

Liu, D., Chen, X., Yue, Y., Chen, M., and Wu, Q. (2011). "Structure and rheology of nanocrystalline cellulose," *Carbohydrate Polymers* 84(1), 316-322. DOI: 10.1016/j.carbpol.2010.11.039

Naumann, A., Navarro-González, M., Peddireddi, S., Kües, U., and Polle, A. (2005). "Fourier transform infrared microscopy and imaging: Detection of fungi in wood," *Fungal Genetics and Biology* 42(10), 0-835. DOI: 10.1016/j.fgb.2005.06.003

Nishimura, H., Kamiya, A., Nagata, T., Katahira, M., and Watanabe, T. (2018). "Direct evidence for α ether linkage between lignin and carbohydrates in wood cell walls," *Scientific Reports* 8(1), 6538. DOI: 10.1038/s41598-018-24328-9

Nwe, N., Furuike, T., and Tamura, H. (2010). "Selection of a biopolymer based on attachment, morphology and proliferation of fibroblast NIH/3T3 cells for the development of a biodegradable tissue regeneration template: Alginate, bacterial cellulose and gelatin," *Process Biochemistry* 45(4), 457-466. DOI: 10.1016/j.procbio.2009.11.002

Roopan, S. M. (2017). "An overview of natural renewable bio-polymer lignin towards nano and biotechnological applications," *International Journal of Biological Macromolecules* 103, 508-514. DOI: 10.1016/j.ijbiomac.2017.05.103

Sakagami, H., Hashimoto, K., Suzuki, F., Ogiwara, T., Satoh, K., Ito, H., Hatano, T., Takashi, Y., and Fujisawa, S. (2005). "Molecular requirements of lignin-carbohydrate

complexes for expression of unique biological activities," *Phytochemistry* 66(17), 2108-2120. DOI: 10.1016/j.phytochem.2005.05.013

Singh, R., Singh, S., Trimukhe, K. D., Pandare, K. V., Bastawade, K. B., Gokhale, D. V., and Varma, A. J. (2005). "Lignin–carbohydrate complexes from sugarcane bagasse: preparation, purification, and characterization," *Carbohydrate Polymers*, 62(1), 57-66. DOI: 10.1016/j.carbpol.2005.07.011

Tang, Y., Yang, S., Zhang, N., and Zhang, J. (2014). "Preparation and characterization of nanocrystalline cellulose via low-intensity ultrasonic-assisted sulfuric acid hydrolysis," *Cellulose* 21(1), 335-346. DOI: 10.1007/s10570-013-0158-2

Uraki, Y., Imura, T., Kishimoto, T., and Ubukata, M. (2004). "Body temperature-responsive gels derived from hydroxypropylcellulose bearing lignin," *Carbohydrate Polymers* 58(2), 123-130. DOI: 10.1016/j.carbpol.2004.05.019

Wang, S., Feng Q., Sun J., Gao F., Fan W., Zhang Z., Li X., and Jiang X. (2015)."Nanocrystalline cellulose improves the biocompatibility and reduces the wear debris of ultrahigh molecular weight polyethylene via weak binding,"v*ACS Nano*, 10(1), 298-306. DOI: 10.1021/acsnano.5b04393

Wang, Z. L., Jia, Y. Y., Shi, Y., Cong, D. L., Chen, Y. Y., Jia, S. R., and Zhou, Y. L. (2009). "Research on characterization and biocompatibility of nano-bacterial cellulose membrane," *Chemical Journal of Chinese Universities* 30(8), 1553–1558 (in Chinese). DOI:10.3321/j.issn:0251-0790.2009.08.015

Wellner, N., Kačuráková, M., Malovíková, A., Wilson, R. H., and Belton, P. S. (1998). "FT-IR study of pectate and pectinate gels formed by divalent cations," *Carbohydrate Research* 308(1–2), 123-131. DOI: 10.1016/S0008-6215(98)00065-2

Xie, Y., Yasuda, S., Wu, H., and Liu, H. (2000). "Analysis of the structure of lignin-carbohydrate complexes by the specific ^{13}C tracer method," *Journal of Wood Science* 46(2), 130-136. DOI: 10.1007/BF00777359

You, T. T., Zhang, L. M., Zhou, S. K., and Feng, X. (2015). "Structural elucidation of lignin-carbohydrate complex (LCC) preparations and lignin from *Arundo donax* Linn," *Industrial Crops and Products* 71, 65-74. DOI: 10.1016/j.indcrop.2015.03.070

Yuan, T. Q., Sun, S. N., Xu, F., and Sun, R. C. (2011). "Characterization of lignin structures and lignin-carbohydrate complex (lcc) linkages by quantitative 13c and 2d hsqc NMR spectroscopy," *Journal of Agricultural and Food Chemistry* 59(19), 10604-14. DOI: 10.1021/jf2031549

Zaman, M., Xiao, H., Chibante, F., and Ni, Y. (2012). "Synthesis and characterization of cationically modified nanocrystalline cellulose," *Carbohydrate Polymers 89*(1), 163-170. DOI: 10.1016/j.carbpol.2012.02.066

Zhang, A., Sun, H., and Wang, X. (2013). "Recent advances in natural products from plants for treatment of liver diseases," *European Journal of Medicinal Chemistry* 63(33), 570-577.DOI: 10.1016/j.ejmech.2012.12.062

Zhang, H., Bai, Y., Zhou, W., and Chen, F. (2017). "Color reduction of sulfonated eucalyptus kraft lignin," *International Journal of Biological Macromolecules* 97, 201. DOI: 10.1016/j.ijbiomac.2017.01.031

Zhao, H., Feng, Q., Xie, Y., Li, J., and Chen, X. (2017a). "Preparation of biocompatible hydrogel from lignin carbohydrate complex (LCC) as cell carriers," *BioResources* 12(4), 8490-8504. DOI: 10.15376/biores.12.4.8490-8504

Zhao, H. K., Li, J. L., Wang, P., Zeng, S. Q., and Xie, Y. M. (2017b). "Lignin-carbohydrate complexes based spherical biocarriers: Preparation, characterization, and biocompatibility," *International Journal of Polymer Science* 2017(2), 1-9. DOI: 10.1155/2017/4915185

Article submitted: March 26, 2019; Peer review completed: May 20, 2019; Revised version received: June 9, 2019; Accepted: June 15, 2019; Published: June 26, 2019.
DOI: 10.15376/biores.14.3.6465-6484